Available online at www.sciencedirect.com
SCIENCE DIRECT®
European Journal of Mechanics B/Fluids 23 (2004) 461–474

Visco-elastic behaviour of suspensions of rigid-rod like particles in turbulent channel flow

Michael Manhart

Fachgebiet Strömungsmechanik, Technische Universität München, Boltzmannstr. 15, 85748 Garching, Germany

Received 1 February 2003; received in revised form 29 July 2003; accepted 30 October 2003

Abstract

Dilute suspensions of rigid elongated particles show visco-elastic behaviour if the particles are small enough to be affected by Brownian motion. The visco-elastic behaviour of such suspensions is investigated in turbulent channel flow. A direct numerical simulation (DNS) of turbulent channel flow has been used to compute Lagrangian time traces of the velocity derivative tensor, as experienced by small inertia-free particles. Along these paths, the viscous and elastic stresses of ensembles of Brownian fibres are computed by a stochastic simulation based on the rheological theory of dilute suspensions of elongated particles and fibres in Newtonian solvents. Average and R.M.S. stresses are computed for various combinations of aspect ratio and Péclet number as a measure for the influence of the Brownian motion. It is found that stress levels as well as R.M.S. of stresses rise quickly with aspect ratio of the particles. The visco-elastic contribution to the total stress level can be as large as 30% for small Péclet numbers showing that elastic effects can indeed take place in suspensions of rigid particles.

1. Introduction

The conditions under which drag reduction due to small amounts of additives can occur in turbulent flows are not yet fully understood. The effect of drag reduction has not only been observed in the context of flexible polymers but also in dilute solutions of surfactants, stiff polymers (Xanthan gum), rigid or flexible fibres and rigid-rod like particles (for an overview, see Gyr and Bewersdorff [1]). The elastic theory of de Gennes [2] that has been later refined by Sreenivasan and White [3] assumes purely elastic effects to be responsible for drag reduction. But, as examples show [4–6], it is possible that there exists another alternative mechanism based on viscous effects acting via the orientation of the suspended fibres or particles, respectively. This is supported by Virk and Wagger [7] who postulate two mechanisms for drag reduction: a type-A and a type-B mechanism. Type B behaviour appears in suspensions in which the polymer molecules are already in a stretched state when the fluid is at rest; in type A drag reduction, the molecules become stretched only due to the action of flow. Both differ significantly in their 'onset' behaviour. Virk and Wagger [7] postulate that in both types of drag reduction only the stretched molecules are active. In order to understand drag reduction mechanisms in polymeric and fibre suspensions, it is therefore important to focus research not only on purely elastic models but also on the rheological behaviour of rigid fibres or particles, respectively. The determining parameters in this context are (i) the elongation ratio and size of the fibres $r = l/d$, (ii) the Reynolds number and (iii) the size of the measuring device. The latter shows that the flow cannot be described by Reynolds similarity only. If the suspended particles are small enough, Brownian motion plays an important role for the dynamics of the suspended microstructure, such that it cannot be neglected in the following considerations.

A considerable body of literature is devoted to the rheological properties of dilute supensions of rigid, neutrally buoyant axisymmetric Brownian particles or fibres suspended in Newtonian liquids. The analytical treatment of dilute particle

E-mail address: michael@flm.mw.tum.de (M. Manhart).

0997-7546/$ – see front matter
doi:10.1016/j.euromechflu.2003.10.013

suspensions in Newtonian fluids starts with the analysis of Einstein [8,9], who derived an expression for the increase of the shear viscosity in the presence of small rigid spheres. Jeffery [10] extended Einstein's theory for small ellipsoidal particles. He analytically derived an equation for the rotary motion and the generated stress field of a small, inertia-free ellipsoidal particle in the Stokes flow limit. From Jeffery's analysis, a rigorous theoretical framework can be derived for the stress field generated in dilute suspensions of sufficiently small particles in a Newtonian solvent [11,12]. Such theory requires that the particles are not interacting with each other. The presence of body forces, Brownian motion or particle interactions can be taken into account by the addition of more terms. Based on this theory, a number of papers appeared dealing with rheological properties of suspensions of spheroids and near spheres in the presence of Brownian rotation [13–19]. Brenner [15] developed a general dynamical rheological theory for axially symmetric particles including spherical dumpbells and long slender bodies with either blunt or bluff pointed ends. According to this framework, the rheological properties of dilute supensions of such bodies, including Brownian diffusion, can be expressed in terms of volume fraction of the suspended particles, the viscosity of the homogeneous Newtonian carrier fluid and five nondimensional scalar material constants which depend only upon the shape of the suspended particles. These material constants are purely hydrodynamic in origin and may be derived from the solution of the quasistatic Stokes equations for a single translating-rotating axisymmetric particle of requisite shape suspended in simple shear flow.

The non-Newtonian stresses in suspensions are dependent on the velocity gradient tensor, the material constants mentioned above and the second and fourth moments of the distribution function of the orientation vector of the suspended particles. Already Jeffery [10] was aware of the problem of finding distribution functions of the orientation angle of the particles. An analytical solution for the orientation distribution function has been found by Okagawa [20] for simple shear flow and vanishing Brownian motion. Brenner [15] provides analytical solutions for steady shear and elongational flows, but there exists no closed solution to this problem in the general case. In such a case, the orientation distribution function has to be computed by numerical means or measured by experimental methods. Examples for experimentally measured orientation angles in shear flow can be found in Frattini and Fuller [21] and Stover et al. [22]. Szeri and Leal [23,24] have developed an efficient double-Lagrangian algorithm for the solution of the Fokker–Planck equation that describes the orientation distribution function of suspended ellipsoidal particles. They applied this algorithm in transient flow problems showing that simple closure strategies for the moments of the distribution function have to be handled with caution.

Applications of numerical methods for the description of suspended Brownian fibres in turbulent flows are rare. Toonder et al. [25] have used a strongly simplified model for the effect of rigid fibres in turbulent pipe flow. This model, based on purely viscous arguments, was able to produce some drag reduction and to modify the turbulence structure in a way that is in line with experimental observations. These results could be confirmed in a direct numerical simulation (DNS) of turbulent channel flow [26]. So far, for a microstructure such as dilute suspensions of Brownian rigid fibres or particles, no macroscopic relations for the stress field generated by the microstructure have been derived, as has been done for elastic dumpbell models by the FENE-P approximation [27]. The FENE-P model, resulting in transport equations for the non-Newtonian stress components, has already been successfully applied in DNS of turbulent channel flow [28–32].

The present paper investigates visco-elastic effects of the rheological behaviour of a dilute suspension of small Brownian particles or fibres in turbulent channel flow. In order to do so, we assume the concentration of the suspension to be small enough that no interaction with the solvent takes place. This allows for computing the orientation distribution function and intrinsic viscosities (stress components) for a great variety of parameters thus quantifying the influence of Brownian motion and aspect ratio of the fibres. The viscous and the elastic contributions of the stress tensor are identified and their contributions to the stress power, i.e., to the exchange of energy between the fibres and the flow, are quantified. We are using DNS for the computation of the velocity gradient tensor along Lagrangian trajectories and a Monte Carlo method for the computation of the moments of the orientation distribution function. In a previous study [33], the algorithms used have been verified for a variety of simple flow cases for which analytical or experimental results are available. In this previous study we investigated the rheological behaviour of dilute suspensions of elongated particles in turbulent channel flow in terms of average and R.M.S. stresses. In the present study, we focus on the visco-elastic behaviour of such suspensions in turbulent channel flow.

The paper is organized as follows. In the next chapter, the rheological theory theory of dilute suspensions of rigid, inertia-free particles is summarized. The numerical schemes used for the DNS and the Monte Carlo simulation are described in Section 3. Section 4.1 presents results for the rheological properties of small Brownian particles in turbulent channel flow. The influence of the Brownian motion on the dynamics of the suspended particles and their visco-elastic properties are investigated in Section 4.2.

2. Theory

2.1. Basic equations

The dynamics of an incompressible fluid consisting of a Newtonian solvent with a minute amount of added polymers can be decribed by the conservation of mass and momentum:

$$\nabla \cdot \mathbf{u} = 0, \tag{1}$$

$$\rho \frac{D\mathbf{u}}{Dt} = -\nabla p + \nabla \cdot \left(\boldsymbol{\tau}^{\mathrm{N}} + \boldsymbol{\tau}^{\mathrm{NN}}\right). \tag{2}$$

Here, $\mathbf{u}$ is the velocity vector, ρ is the density and p is the pressure. $\boldsymbol{\tau}^{\mathrm{N}}$ is the part of the stress tensor attributed to the Newtonian solvent and $\boldsymbol{\tau}^{\mathrm{NN}}$ is the non-Newtonian part of the stress tensor due to the suspended particles. For the Newtonian part of the stress tensor $\boldsymbol{\tau}^{\mathrm{N}}$ the following constitutive equation is generally accepted:

$$\boldsymbol{\tau}^{\mathrm{N}} = 2\mu \mathbf{D}, \tag{3}$$

where μ is the dynamic viscosity and $\mathbf{D}$ is the rate-of-strain tensor

$$\mathbf{D} = \left(\nabla \mathbf{u} + \nabla \mathbf{u}^{\mathrm{T}}\right)/2. \tag{4}$$

For the contribution of the polymeric molecules to the stress tensor $\boldsymbol{\tau}^{\mathrm{NN}}$, a non-Newtonian constitutive relation has to be supplied. The stresses caused by the presence of particles is a function of the moments of their orientation distribution function. The orientation distribution function is a probability density function of the orientation angle which is determined by the dynamics of the particles. If the paricles are sufficiently small, their dynamics will be affected by Brownian motion, which results in a stochastic differential equation for the dynamics of small Brownian particles.

2.2. Evolution equation for a single Brownian particle

An equation for the orientation vector $\mathbf{n}$ of rigid ellipsoidal particles in shear flow has been derived by Jeffery [10] under the assumption of small particle Reynolds numbers, i.e., Stokes flow:

$$\frac{D\mathbf{n}}{Dt} = \boldsymbol{\Omega} \cdot n + \kappa\left[\mathbf{D} \cdot \mathbf{n} - (\mathbf{n} \cdot \mathbf{D} \cdot \mathbf{n})\mathbf{n}\right], \tag{5}$$

where $\boldsymbol{\Omega}$ is the vorticity tensor. The material constant κ indicates the shape of the particle, and is determined by

$$\kappa = \frac{r^2 - 1}{r^2 + 1}, \tag{6}$$

where r is the aspect ratio of the particle.

If $\kappa = 0$, the particles have a spherical shape and rotate with the average rotation rate of the fluid as indicated by the term $\boldsymbol{\Omega} \cdot \mathbf{n}$. If $\kappa \to 1$, the particles behave like slender rods. This equation holds not only for ellipsoidal particles but is valid for other axisymmetric particles. The shape of the particle enters Eq. (5) by a modified shape factor κ [15].

If the mass of a particle immersed in a fluid is small enough then it is subjected to Brownian motion due to the thermal fluctuations of the surrounding molecules. The Brownian motion of a particle is a random process if considered on the time and length scales of continuum mechanics and can be modelled in the evolution equation of the orientation of a small particle as a random force term $\boldsymbol{\Gamma}(t)$ added to Eq. (5):

$$\frac{D\mathbf{n}}{Dt} = \boldsymbol{\Omega} \cdot \mathbf{n} + \kappa\left[\mathbf{D} \cdot \mathbf{n} - (\mathbf{n} \cdot \mathbf{D} \cdot \mathbf{n})\mathbf{n}\right] + \boldsymbol{\Gamma}(t). \tag{7}$$

The random force term $\boldsymbol{\Gamma}$ is proportional to the Langevin force $\mathbf{F}_f(t)$ divided by the mass m of the particle:

$$\boldsymbol{\Gamma}(t) = \mathbf{F}_f(t)/m. \tag{8}$$

The noise strength of the Langevin force is given by

$$\left\langle \boldsymbol{\Gamma}(t)\boldsymbol{\Gamma}(t)\right\rangle = q\delta(t - t'), \tag{9}$$

i.e., it is uncorrelated over different times. With the Boltzmann constant k_b, the friction coefficient γ and the temperature T it is given by

$$q = 2\frac{k_b T}{\gamma m^2}. \tag{10}$$

Table 1
Péclet numbers for fibre suspensions in turbulent channel flow of water ($Re_b = 40\,000$, temperature of 293 K, channel height $D = 0.1$ m)

Length in m	10^{-6}	10^{-5}	10^{-4}	10^{-3}
Péclet number	3.8×10^{-1}	3.8×10^{2}	3.8×10^{5}	3.8×10^{8}

For the rotation of an axisymmetric particle about its transverse axis, the friction coefficient is given by Brenner [15]

$$\gamma = 6V_p\mu_0 K_T \tag{11}$$

with μ_0 being the viscosity of the Newtonian solvent V_p being the particle volume and K_T being a material constant.

The Langevin force has a formal representation as the increment of a Wiener process

$$\mathbf{F}_f(t) = \sqrt{\frac{2k_bT}{\gamma}}\,\frac{\partial \mathbf{W}}{\partial t} \tag{12}$$

with the diffusion coefficient $D_r = k_bT/\gamma$ [34].

The distribution function $\Psi(\mathbf{n}, t)$ that describes the fraction of particles in a fluid element which have orientation vectors residing around $\mathbf{n}$ at time t is determined by a Fokker–Planck equation.

$$\frac{\partial \Psi}{\partial t} = -\nabla \cdot \left(\Psi \frac{\partial \mathbf{n}}{\partial t}\right) + \frac{\partial^2}{\partial \mathbf{n}^2} D_r \Psi. \tag{13}$$

This is essentially a conservation equation in orientation space. It was first used by Fokker and Planck to describe the Brownian motion of small particles. It consists of a drift term $\nabla \cdot (\Psi \frac{\partial \mathbf{n}}{\partial t})$ and the Brownian diffusion term $\frac{\partial^2}{\partial \mathbf{n}} D_r \Psi$.

The non-dimensional number characterizing the importance of the Brownian term in relation to the velocity gradient is the Péclet number

$$Pe = \frac{\partial u/\partial x}{D_r} \tag{14}$$

in which $\partial u/\partial x$ is a characteristic shear rate. Eq. (11) tells us that the Péclet number increases linearly with the volume of the particles. Consider a turbulent channel flow of water with the following parameters: channel height $D = 0.1$ m; bulk velocity $u_b = 0.4$ m/s; $Re_b = 40\,000$, temperature of 293 K. If particles of aspect ratio $r_p = 50$ are suspended, then the Péclet numbers are dependent on the length of the particles as given in Table 1. This example shows that particles in the micrometer range are required to achieve Péclet numbers below 100, in this specific configuration. If the size of the apparatus is increased, the Péclet number decreases quadratically with the channel height.

2.3. The constitutive equation based on rigid-rod like particles

The stress field caused by an ensemble of rigid particles can be integrated over stress fields generated by single particles if the suspension is sufficiently dilute [12]. All relevant Reynolds numbers based on particle size and translational and rotational velocities and shear rate are assumed to be small compared to unity to justify neglecting nonlinear terms in the Navier–Stokes equations. In such a case, the flow in the presence of suspended particles is supposed to be governed by the quasistatic creeping motion equations, which are linear. In consequence of the linearity, the hydrodynamic force **F**, torque **L** and stresslet **A** (compare Batchelor [12]) exerted by the fluid on the particle are linear functions of the translational slip velocity , the rotational slip velocity and the shear of the fluid in the neighbourhood of the particle. In the general case of arbitrarily shaped particles, **F**, **L** and **A** can therefore be related to the translational and rotational slip velocities and the shear rate via material tensors, which are intrinsic properties of the particle alone, being dependent only upon its size and shape. Inertia-free particles, i.e. particles with the same density as the solvent, are convected with the fluid velocity such that translational and rotational slip velocities are zero. In such a case, the hydrodynamic force **F** and torque **L** on the particle are zero. For particles with a center of symmetry, only five material constants are required [15] which are dimensionless and therefore independent upon the size of the particle. These constants can be derived by solving the equations of motion of quasistatic creeping flow around the particle. Brenner [15] tabulates these constants for spheroids, long slender axisymmetric bodies and dumbbells, all of which can be derived analytically (e.g., Giesekus [11]).

Suppose that the suspended particle is inertia-free, i.e., it is force free and couple free. Then, the hydrodynamic force and torque are zero. For a centrally-symmetric body it then follows [15] that the translational slip velocity is zero and the angular slip velocity is a linear function of the shear rate.

In a suspension of particles, each fluid element contains a large number of particles with varying orientations. The macroscopic stress due to this number of particles is obtained by averaging over a large number of individual particles

$$\boldsymbol{\tau}^{\mathrm{NN}} = 2\mu_0\mathbf{D} + \mu_1\mathbf{ID} : \langle\mathbf{nn}\rangle + \mu_2\mathbf{D} : \langle\mathbf{nnnn}\rangle + 2\mu_3\big(\langle\mathbf{nn}\rangle\cdot\mathbf{D} + \mathbf{D}\cdot\langle\mathbf{nn}\rangle\big) + 2\mu_4 D_r\big(3\langle\mathbf{nn}\rangle - \mathbf{I}\big) \tag{15}$$

involving the second moment $\langle\mathbf{nn}\rangle$ and the fourth moment $\langle\mathbf{nnnn}\rangle$ of the distribution function of the orientation vector. The material coefficients $\mu_0,\ldots,\mu_4$ are linear functions of the volume fraction of the particles. For a rigorous derivation of this constitutive equation, the papers of Giesekus [11], Batchelor [12], Brenner [15] or Hinch and Leal [19] may be useful.

The moments arise from an ensemble-averaging of the effects of a large number of individual particles, each of them having a different orientation angle. The determination of non-Newtonian stresses involves the knowledge or estimation of the moments of the distribution function of the microstructural conformation.

2.4. Visco-elastic behaviour

The stress tensor $\boldsymbol{\tau}^{\mathrm{NN}}$ consists of two terms, a viscous and an elastic contribution (compare Doi and Edwards [35]):

$$\boldsymbol{\tau}^{\mathrm{NN}} = \boldsymbol{\tau}^{\mathrm{V}} + \boldsymbol{\tau}^{\mathrm{E}}, \tag{16}$$

where the viscous stress is proportional to the current strain rate tensor

$$\boldsymbol{\tau}^{\mathrm{V}} = 2\mu_0\mathbf{D} + \mu_1\mathbf{ID} : \langle\mathbf{nn}\rangle + \mu_2\mathbf{D} : \langle\mathbf{nnnn}\rangle + 2\mu_3\big(\langle\mathbf{nn}\rangle\cdot\mathbf{D} + \mathbf{D}\cdot\langle\mathbf{nn}\rangle\big) \tag{17}$$

and the elastic stress is given by

$$\boldsymbol{\tau}^{\mathrm{E}} = 2\mu_4 D_r\big(3\langle\mathbf{nn}\rangle - I\big). \tag{18}$$

Phenomenologically, the viscous stress is the stress which vanishes instantaneously when the flow is stopped. The elastic stress does not vanish until the system is in equilibrium. It describes the stresses due to the Brownian motion. It is the only term that results in stresses that are not linearly dependent on the deformation rate tensor of the surrounding fluid, i.e., it results in stresses remaining in a fluid at rest. It is a consequence of the relaxation of the distribution function towards its isotropic equilibrium due to Brownian motion. This equilibrium is described by the diagonal elements of $\langle\mathbf{nn}\rangle$ taking the value 0.33. One can easily verify that the Brownian stress term will disappear under this equilibrium. The consequences of the Brownian stresses are severe. They change the material properties from a purely viscous behaviour to visco-elastic behaviour if the Brownian motion is large enough, i.e., the particles are small enough to be subjected to the Brownian motion. The ensemble of particles will then be able to store energy and release it again at a later instant of time. This energy will be released to the surrounding fluid via the relaxation process described by the elastic stress. It is the purpose of this paper to investigate the relative importance of the elastic stress in comparison to the viscous stresses and to evaluate under which conditions visco-elastic effects can play a role in suspensions of non-elastic materials.

The energy exchange between the solvent and the supended particles is described by the stress power S_p which according to Eq. (16) consists of a viscous and an elastic term,

$$S_p = \boldsymbol{\tau}^{\mathrm{NN}}\cdot\mathbf{D} = \Phi + \frac{DA^{\mathrm{P}}}{Dt}. \tag{19}$$

The viscous term is related to the additional hydrodynamic energy dissipation Φ due to the presence of the fibres.

$$\Phi = \boldsymbol{\tau}^{\mathrm{V}}\cdot\mathbf{D}. \tag{20}$$

The elastic term is related to the change in the free energy A^{P} of the fibre system due to the exchange with the solvent

$$\frac{DA^{\mathrm{P}}}{Dt} = \boldsymbol{\tau}^{\mathrm{E}}\cdot\mathbf{D}. \tag{21}$$

While the energy dissipation is always positive, the rate of change of free energy can be positive or negative, which accounts for accumulation or release of free energy, respectively.

3. Numerical method

The rheological properties of a suspension of small fibres in turbulent channel flow are investigated by coupling of two different simulation methods. The turbulent flow field on the macroscopic level is provided by a direct numerical simulation (DNS). The conformation of the fibres is computed by a particle simulation using information of the time dependent velocity derivative tensor seen by a fluid element traveling with the flow in a Lagrangian framework.

Table 2
Grid parameters for the DNS of turbulent channel flow $Re_\tau = 180$

NX	NY	NZ	Δx^+	Δy^+	$\Delta z^+_{\min}$
96	80	64	18.0	13.5	2.7

3.1. DNS of turbulent channel flow

Our DNS method for the solution of Eqs. (1) and (2) uses an explicit version of the projection or fractional step method proposed independently by Chorin [36] and Temam [37]. We use a Leapfrog scheme for the explicit time advancement of the momentum equation. The flow variables are defined on a non-equidistant Cartesian mesh in a staggered arrangement [38]. The specific discrete formulations are derived by integrating the equations over the corresponding control cells surrounding the definition points of the individual variables. We are using the mid-point rule for approximating the fluxes by the variables. The required interpolations and the approximation of the first derivatives are performed by fourth order compact interpolation and difference formulations, respectively [39]. The Poisson equation is solved by a direct method using Fast-Fourier transformations in the homogeneous streamwise and spanwise directions of the channel flow and a tridiagonal solver in the wall-normal direction.

The integration of the particle paths is done by an Euler time step using fourth order interpolation for the velocities. The velocity derivative tensor is estimated at the instantaneous positions of the particles by a fourth order difference formula which ensures a continuous velocity derivative tensor in time.

The DNS of turbulent channel flow is well documented in Manhart and Friedrich [26]. We performed grid resolution studies and evaluated the influence of the discretisation order on the results. Our results have been verified against the highly accurate results of the spectral simulations of Kim et al. [40]. These tests showed that the numerical grid listed in Table 2 was sufficiently accurate to investigate the dynamics of suspensions of Brownian particles in turbulent channel flow.

3.2. Stochastic simulation of the conformation distribution function

We use a stochastic simulation method (Monte Carlo simulation) to compute the distribution function $\Psi(\mathbf{n}, t)$ of the orientation angle of the suspended particles. To do so, the Jeffery equation (5) is integrated for a sufficient number of particles using the derivative tensor obtained by the DNS of turbulent channel flow. For time advancement, an Euler time step is used. Numerical tests show, that the conformation distribution function is relatively insensitive against the time stepping. The Brownian term is modelled by a stochastic Wiener process with a Gaussian distribution, which itself is modeled by a random number generator. In combination with an Euler time step, it is sufficient to use random numbers with uniform distribution as increments of the Wiener process [34]. The strength of the random force in a uniform distribution B_{uni} is connected to the one with a Gaussian distribution B by

$$B_{\text{uni}} = \sqrt{12\Delta t}\, B. \tag{22}$$

The intensity B of the random numbers is connected to the Brownian diffusivity by

$$B = \sqrt{2D_r}. \tag{23}$$

A detailed verification of the stochastic simulation method for the microstructure can be found in Manhart [33]. The Monte Carlo method is verified using analytical results for non-Brownian particles in simple shear flow [20], experimental results of orientation distribution functions of Brownian particles in simple shear flow [21] and analytical results from rheological theory of dilute suspensions of Brownian particles in simple steady flows [15]. The tests showed that the stochastic simulation method is able to predict the orientation distribution function and the corresponding results from rheological theory of small Brownian particles suspended in a Newtonian solvent in uniform shear flow.

4. Results

In order to study the rheological behaviour and visco-elastic effects in turbulent channel flow, we extracted time records of position $X(t)$ and velocity gradients $\nabla\mathbf{u}(t)$ as seen by small inertia-free fluid-particle in a Lagrangian framework from a DNS of turbulent channel flow ($Re_\tau = 180$). These time records have been used to solve Jeffery's equation for ensembles of Brownian particles and determining intrinsic stresses generated by these suspended particles. We have stored 4000 time steps corresponding to a total time of $t \cdot u_b/h = 40$. During this time, a virtual fluid-particle is convected four times through the whole computational domain (using u_b). Having stored 10 000 of such Lagrangian time traces, we have 40×10^6 data points

for building averages. For the calculation of the moments of the conformation tensor and the stresses, we used 500 particles along each Lagrangian path. It has been found that this number is sufficient to keep the error norm with respect to a reference solution with 5000 particles below 2×10^{-4}.

4.1. Average and R.M.S. stresses in dilute fibre suspensions in turbulent channel flow

Detailed results concerning average stresses and their corresponding R.M.S. values have been presented in Manhart [33]. In the following, we show some representative results and a short summary of the findings of this previous paper. Figs. 2–5 show

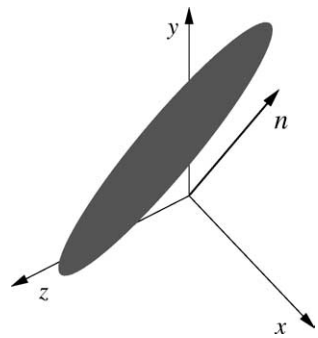

Fig. 1. Configuration of a rigid-rod-type macromolecule.

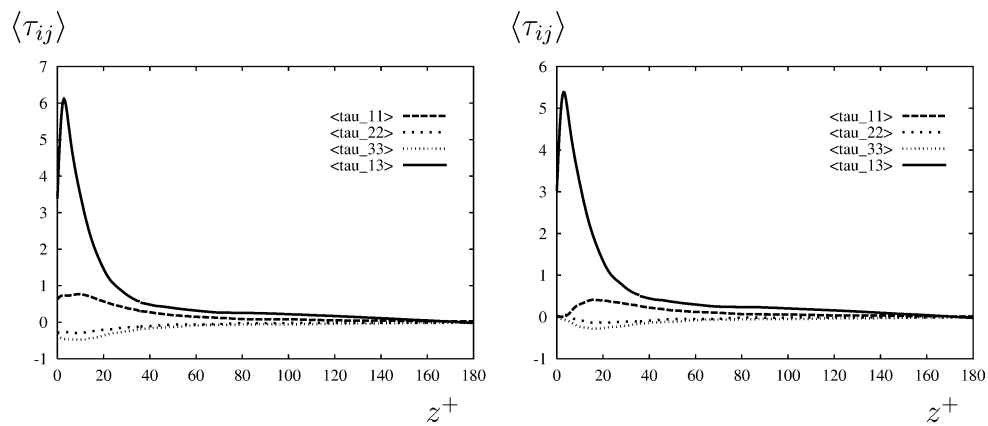

Fig. 2. Average non-Newtonian stresses in turbulent channel flow for ellipsoidal particles ($r = 10.0$); $Pe = 98$ (left);$Pe = 383000$ (right).

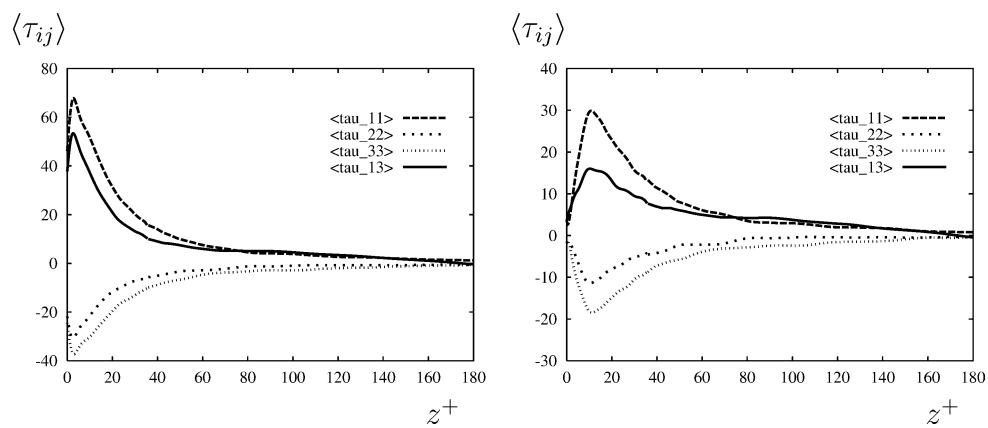

Fig. 3. Average non-Newtonian stresses in turbulent channel flow for ellipsoidal particles ($r = 100.0$); $Pe = 98$ (left); $Pe = 383000$ (right).

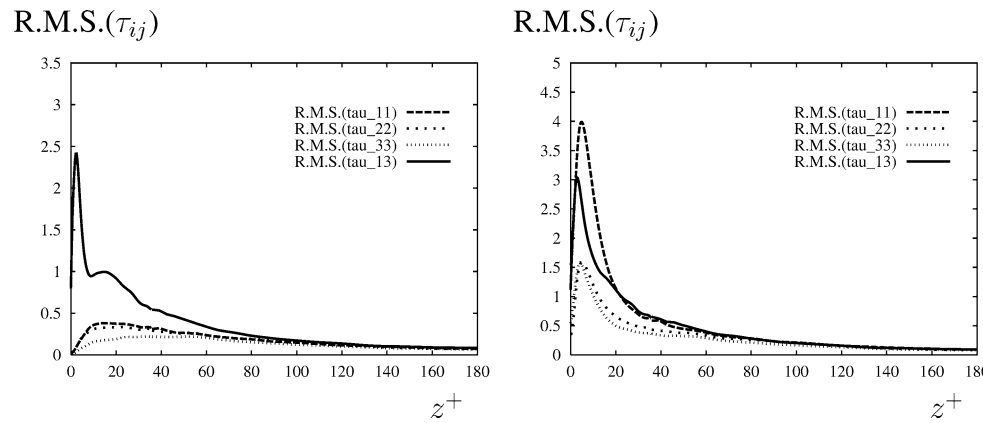

Fig. 4. R.M.S. of non-Newtonian stresses in turbulent channel flow for ellipsoidal particles ($r = 10.0$); $Pe = 98$ (left); $Pe = 383000$ (right).

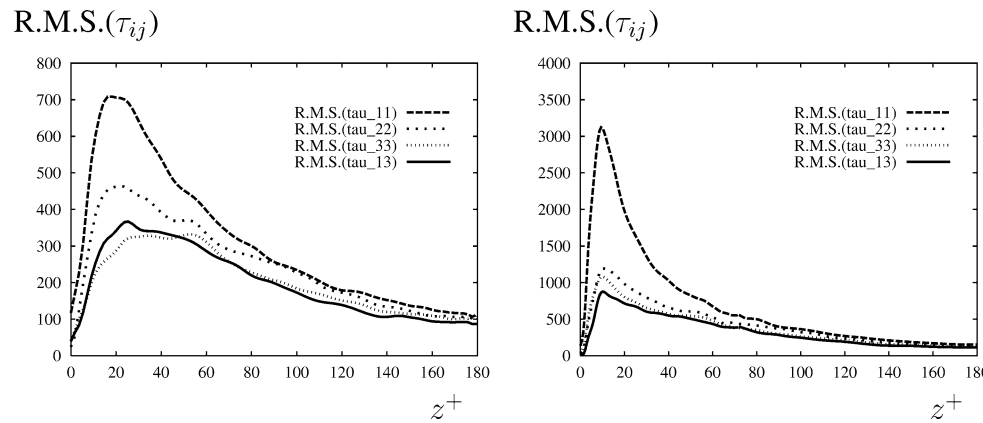

Fig. 5. R.M.S. of non-Newtonian stresses in turbulent channel flow for ellipsoidal particles ($r = 100.0$); $Pe = 98$ (left); $Pe = 383000$ (right).

average and R.M.S. stresses in turbulent channel flow at aspect ratios $r = 10.0$ and $r = 100.0$ as well as Péclet numbers of $Pe = 98$ and $Pe = 383000$. In what follows, we always show intrinsic stresses for vanishing concentration, which are expressed in terms of unit volume fraction ϕ.

The peaks of the non-Newtonian stresses can be found in the buffer layer. The shorter fibres ($r = 10$) generate large shear stresses (Fig. 2) and the normal stresses remain small compared to the shear stresses. With the longer fibres ($r = 100$, Fig. 3), the normal stresses and stress differences exceed the shear stress magnitude. Fibres with aspect ratios above $r \approx 100$ generate qualitatively the same mean and R.M.S. stress distributions. This is due to the fact that the dynamics of the suspended particles determined by Eq. (7) remains essentially the same for large aspect ratios, because κ tends to unity. The overall magnitude of the stresses rises strongly with the aspect ratio of the fibres. The stress levels scale with r^2 when keeping the volume fraction constant. This result is a confirmation of the experimental observation that large-aspect ratio fibres are more effective in modifying the turbulence structure than small-aspect ratio fibres, because long fibres need a smaller volume fraction to generate the similar stress distributions as short fibres do. The non-Newtonian character of the suspension, as it is expressed by the appearance of normal stress differences, is also stronger for large-aspect ratio fibres.

The Brownian motion plays an important role for the stress levels and distributions. The average stresses are enhanced by Brownian fluctuations. That means that smaller fibres with smaller Péclet number lead to higher average stress levels than larger fibres do. But the r.m.s. values of the stresses are reduced by Brownian motion. That means that smaller fibres lead to lower stress fluctuation levels in the suspension. In all cases it is observed that the Brownian motion moves the average stress peaks towards the wall.

The average shear stress of the fibres enters directly the streamwise momentum balance in turbulent channel flow in addition to the viscous and turbulent stresses. It can be related to the so-called “stress deficit”, which has been observed in many experiments under drag reducing conditions (see Gyr and Bewersdorff [1]). There are suggestions that the high extensional viscosities are the principal instrument in reducing the drag [41]. The high extensional viscosities are equivalent with high

normal stresses. Longer fibres produce smaller average shear stresses in comparison to the normal stresses than shorter fibres do. By considering this, it might be more likely that longer fibres are more effective in reducing turbulent drag.

4.2. Visco-elastic behaviour

The elastic contribution to the stress tensor is given by Eq. (18). The elastic stress is linearly dependent on the second moment of the distribution function $\langle \mathbf{nn} \rangle$. The strength is determined by the material coefficient μ_4, volume fraction and the Brownian diffusivity D_r. We therefore investigate first the behaviour of $\langle \mathbf{nn} \rangle$ at various Péclet numbers in simple shear flow and turbulent channel flow. Fig. 6 shows $\langle n_1 n_1 \rangle$ in simple shear flow after a sudden start of the shearing. If the Péclet number is small, the Brownian term dominates the dynamics of the particles and the orientation angles remain homogeneously distributed which is indicated by $\langle n_1 n_1 \rangle = 0.\overline{3}$. With increasing influence of the shearing, i.e., with increasing Péclet number, the particles tend to align and to reach a statistically stationary orientation that is obtained for $Pe < 100$. At larger Pe, the Brownian motion is no longer sufficiently strong to keep the distribution in a statistically stationary state and periodic oscillations set in. At $Pe = \infty$, these oscillations are described by the analytical solution of Okagawa et al. [20].

The moments behave similarly in turbulent channel flow at low values of the Péclet number, i.e., the Brownian fluctuations are strong enough to enforce a statistically stationary state of the orientation of the particles (Fig. 7). But this state ceases at smaller Péclet number than in the simple shear flow. This is because the turbulent fluctuations generate strong oscillation of the velocity gradient tensor. At high Péclet numbers, the particles follow these oscillations very rapidly as seen in Fig. 7 (right). We have verified that the observed peak at $t = 12$ is not connected to the periodic solution observable in simple shear flow, but is a response to the turbulent velocity field.

In the following we analyse the behaviour of the stresses generated by the particles in various configurations. We computed the viscous and elastic stresses τ^{V} and τ^{E}, respectively, in order to quantify their contributions to the total non-Newtonian

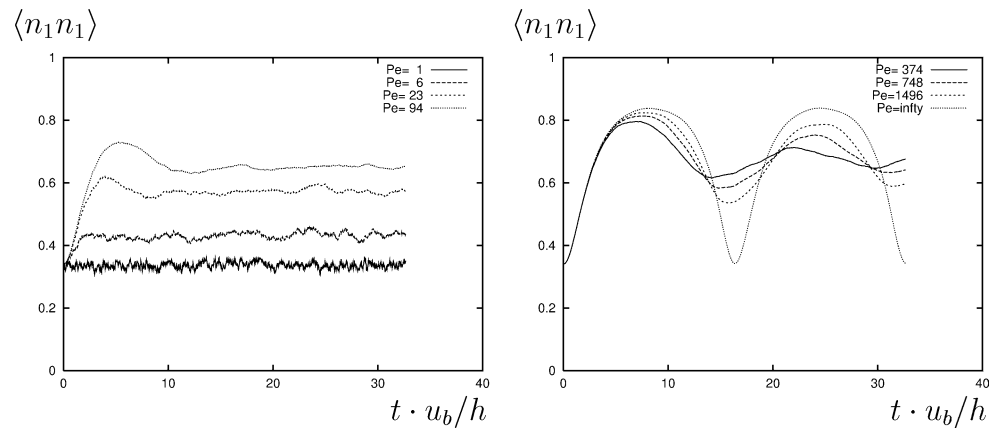

Fig. 6. Influence of the Péclet number on the second moment $\langle n_1 n_1 \rangle$ in simple shear flow ($r = 5.6$).

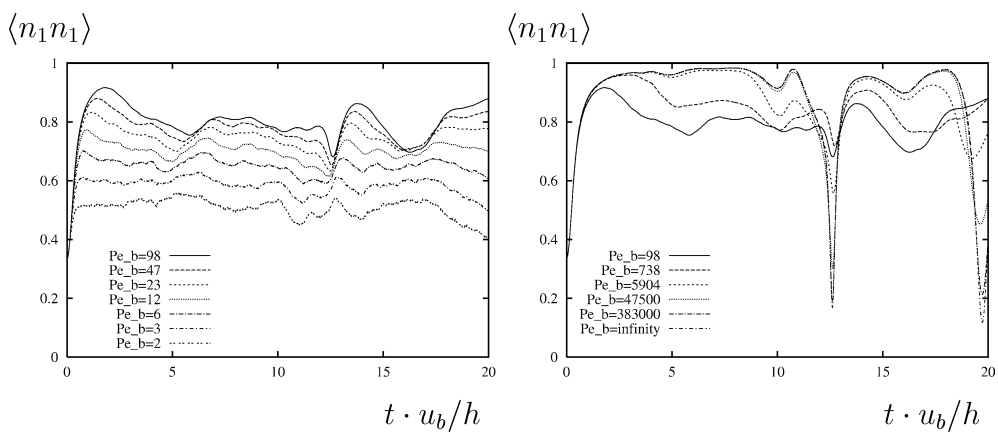

Fig. 7. Influence of the Péclet number on the second moment $\langle n_1 n_1 \rangle$ in turbulent channel flow ($r = 5.6$).

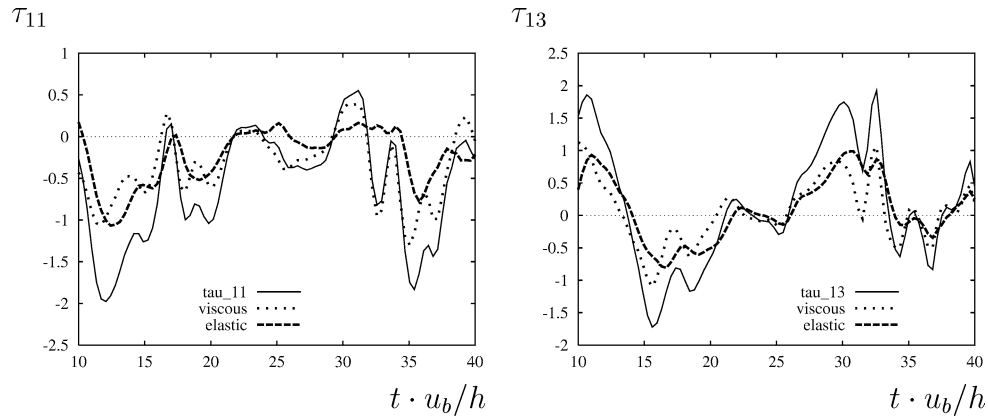

Fig. 8. Non-Newtonian stresses in turbulent channel flow along one Lagrangian path ($r = 20.0,\ Pe = 10.0$); τ_{11} (left); τ_{13} (right).

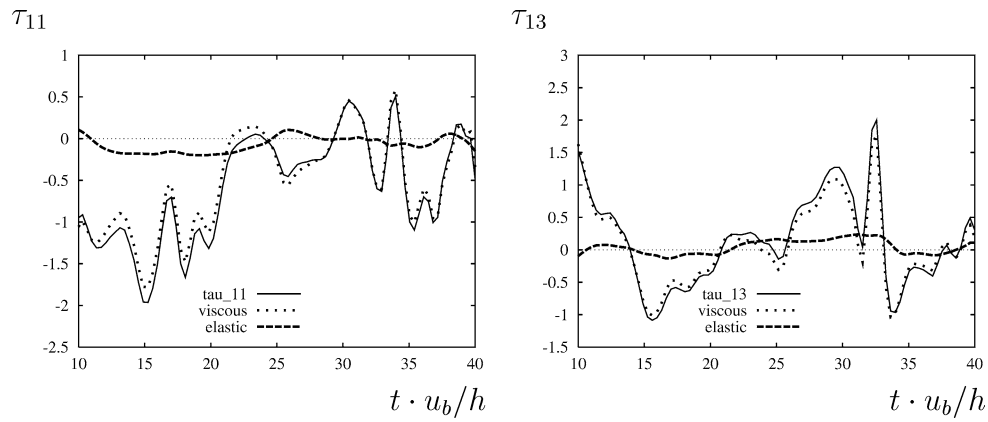

Fig. 9. Non-Newtonian stresses in turbulent channel flow along one Lagrangian path ($r = 20.0,\ Pe = 98.0$); τ_{11} (left); τ_{13} (right).

stress. We first show time traces of the primary normal and shear stresses τ_{11} and τ_{13} along an arbitrary Lagrangian particle path. The aspect ratio was set to $r = 20.0$ for these tests. In Fig. 8, we show the time traces for $Pe = 10$ and in Fig. 9 those for $Pe = 98$. These figures illustrate the increasing importance of the visco-elastic stress contribution with decreasing Péclet number. At $Pe = 10$, there is a significant contribution of the elastic term to the non-Newtonian stresses. At $Pe = 98$, the elastic stress has only a vanishing contribution. The elastic contribution changes the total stress at $Pe = 10$ not only quantitatively, but also qualitatively. This is due to a phase shift observable in the elastic with respect to the viscous stress.

The stress power is plotted in Fig. 10 (left) for $Pe = 10$ and $r = 20.0$. There are significant contributions of the elastic stresses. At the moment, it seems that both elastic and viscous stress power are positive most of the time, indicating a net energy transfer from the solvent to the fibre system. In this context, we like to mention the investigation of a FENE-P model under drag reducing conditions by de Angelis et al. [30]. They found that in the configuration investigated, the polymer behaviour was essentially dissipative, i.e., the stress power remained positive most of the time. In Fig. 10 (right), we show the individual contributions from the three velocity components u_i to the elastic stress power,

$$S_p(u_i) = \tau^{\mathrm{E}}_{(i)k}\partial\frac{u_{(i)}}{\partial x_k}. \tag{24}$$

There are instants in time where the stress power is negative for one component and positive for the others. This means, that at the same instant, energy is taken from one velocity component and released to another one.

The average and R.M.S. contributions of the elastic stress for $r = 20.0$ can be inferred from Figs. 11–14. While the elastic shear stresses remain small, the average elastic normal stresses reach about one third of the total normal stresses for $Pe = 10$ and about 10% for $Pe = 98$. The average elastic normal stresses share the same qualitative behaviour with the total stresses. This is not the case for the R.M.S. of the stresses. The R.M.S. of τ_{11} and τ_{13} show a near wall peak at $Pe = 10$ not being present in the elastic stresses. The contribution of the elastic to the total stresses is between 10% and 20% for $Pe = 10$ but below 1% for $Pe = 98$.

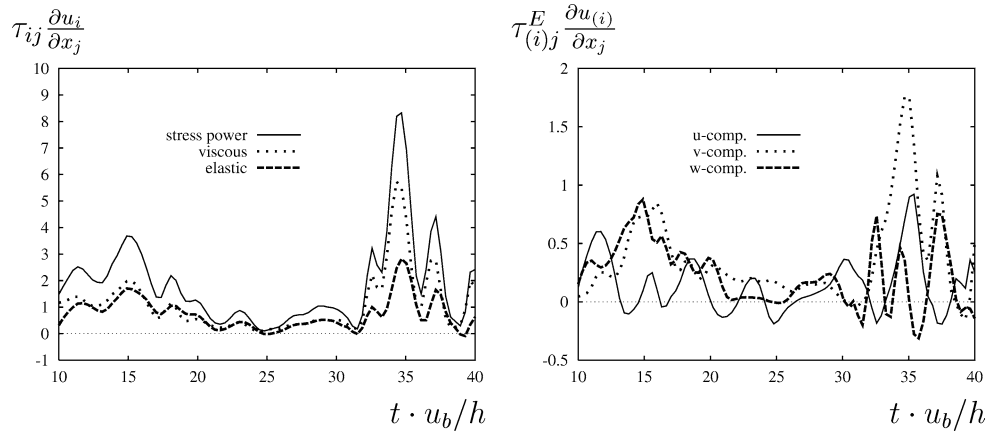

Fig. 10. Stres power in turbulent channel flow along one Lagrangian path ($r = 20.0,\ Pe = 10.0$); full stress power $\tau_{ij}\partial u_i/\partial x_j$ (left); elastic contributions of individual velocity components $\tau^{\mathrm{E}}_{(i)j}\partial u_{(i)}/\partial x_j$ (right).

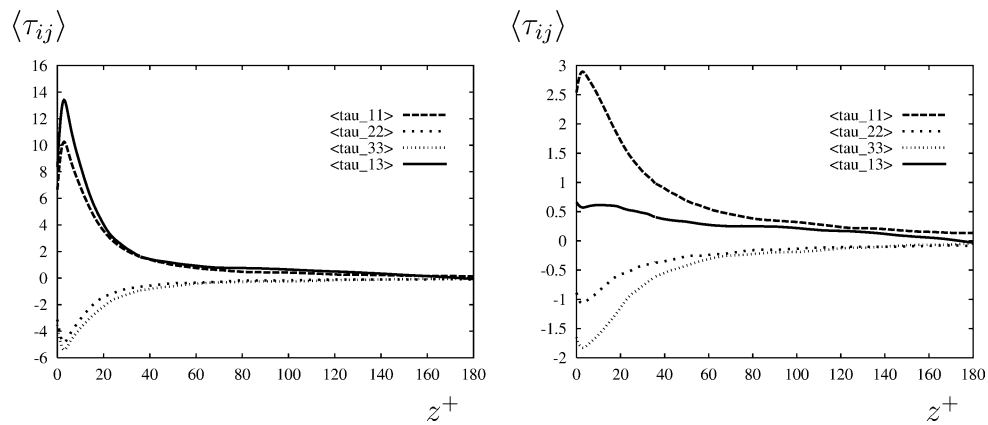

Fig. 11. Average non-Newtonian stresses in turbulent channel flow for ellipsoidal particles ($r = 20.0$); $Pe = 10$ (left); contribution of Brownian term (right).

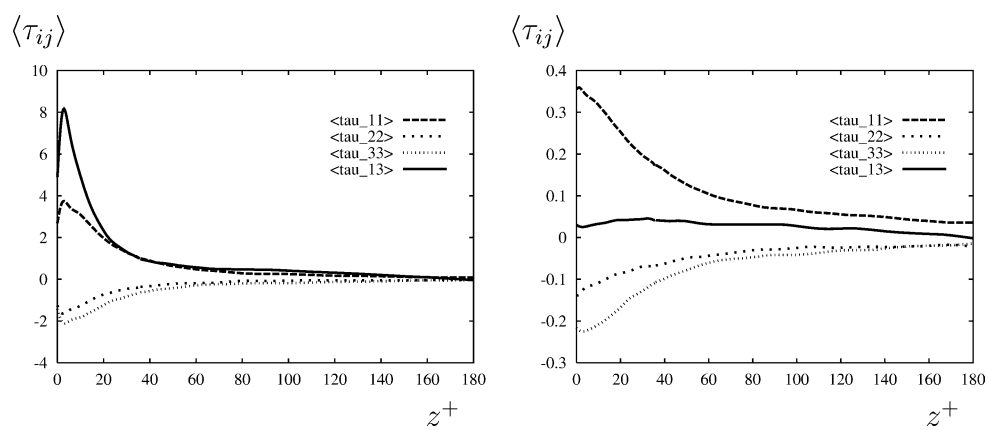

Fig. 12. Average non-Newtonian stresses in turbulent channel flow for ellipsoidal particles ($r = 20.0$); $Pe = 98$ (left); contribution of Brownian term (right).

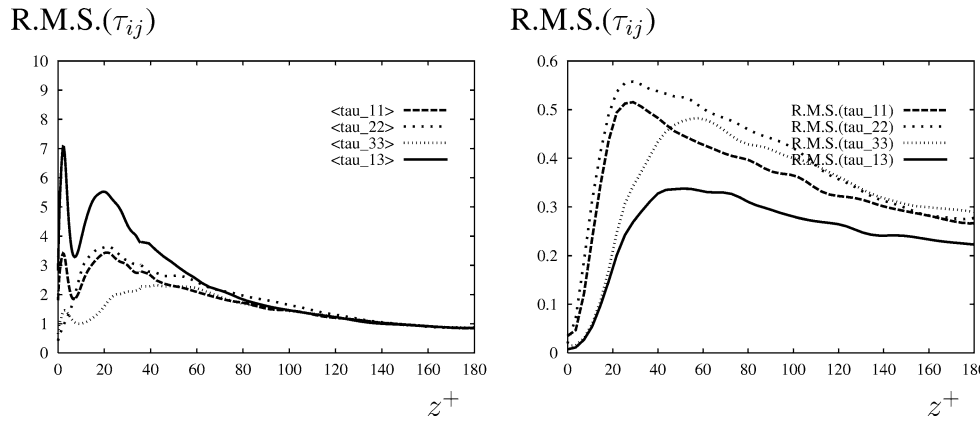

Fig. 13. R.M.S. of non-Newtonian stresses in turbulent channel flow for ellipsoidal particles ($r = 20.0$); $Pe = 10$ (left); contribution of Brownian term (right).

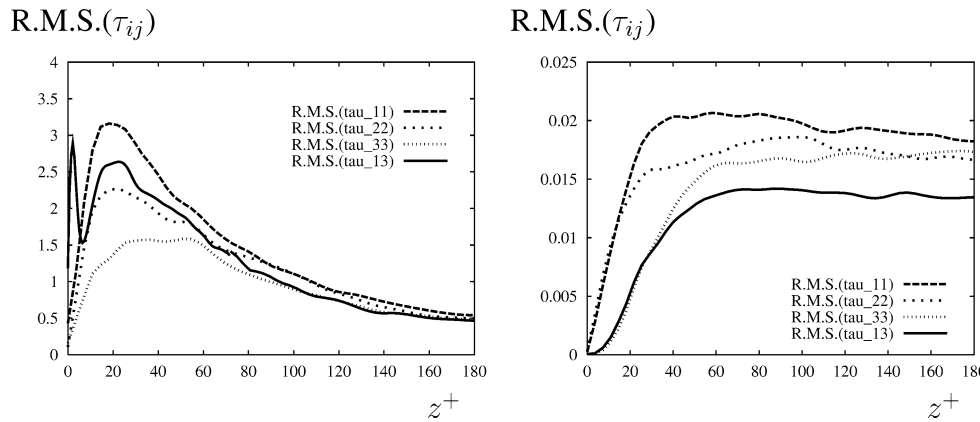

Fig. 14. R.M.S. of non-Newtonian stresses in turbulent channel flow for ellipsoidal particles ($r = 20.0$); $Pe = 98$ (left); contribution of Brownian term (right).

5. Conclusions

Dilute suspensions of small, Brownian rigid-rod like particles, resp. fibres in Newtonian solvents are able to show visco-elastic behaviour. We have investigated visco-elastic effects in turbulent channel flow at $Re_\tau = 180$ by numerical means. Lagrangian trajectories have been computed by a DNS of the Newtonian solvent. Along these trajectories, the microscopic equations describing the conformation and rheology of fibres of various size and elongations have been computed by a Monte Carlo method. The numerical schemes have been validated for simple shear and extensional flows [33].

The suspended particles generate non-Newtonian stresses primarily in the buffer layer. The overall magnitude of the stresses rises strongly with the aspect ratio of the fibres. There are arguments for the importance of high extensional viscosities, i.e., normal stresses, to be the principal instrument in reducing the drag [41]. If strong normal stresses are responsible for drag reduction, these go in hand with a considerable average shear stress. The average shear stress enters the streamwise momentum balance and has to be compensated by a reduction of the primary Reynolds shear stress. This shear stress is smaller with longer fibres than with shorter fibres. This consideration shows that it is more likely to achieve drag reduction with longer fibres than with short ones.

The Brownian motion is an important factor for the magnitude, the distribution and the character of the stresses. It is able to produce visco-elastic behaviour if the particles are small enough to be subjected to the Brownian motion. We showed that the behaviour of the second moment of the distribution function of the particles' orientation tensor is altered significantly with the influence of the Brownian motion. At small Péclet number, the Brownian motion is strong enough to enforce a statistically stationary distribution of the suspension. The elastic contribution to the stresses is increasingly important with smaller Péclet numbers. About 30% of the total stress level is due to the elastic contribution in a configuration of $r = 20$ and $Pe = 10$.

The elastic stresses show a phase shift with respect to the viscous stresses that are linearly dependent on the strain-rate tensor. This phase shift leads to qualitative changes in the stress history with respect to cases with higher Péclet numbers which could lead to a release of stored energy from the fibre system to the solvent. The overall behaviour of the fibre system seems however to be dissipative as also observed by Angelis et al. [30] in a FENE-P model for elastic polymers. When looking at energy fluxes from individual velocity components to the fibre system, we observe significant backward energy transfer from the fibres to one or the other velocity component. Energy is taken from one component and released to the other at one instant of time. One might be attempted to speculate that this establishes a mechanism responsible for energy redistribution among the three velocity components, which could be responsible for increased Reynolds stress anisotropies observed under drag reducing conditions. Final conclusions can however only be drawn if simulations with full coupling between fibre stresses and solvent are available.

Acknowledgements

This work has been supported by the Deutsche Forschungsgemeinschaft (DFG, Sonderforschungsbereich 438). We also gratefully acknowledge the support by the Leibniz Computing Centre (LRZ) of the Bavarian Academy of Sciences

References

[1] A. Gyr, H.-W. Bewersdorff, Drag Reduction of Turbulent Flows by Additives, in: Fluid Mech. Appl., vol. 32, Kluwer Academic, Dordrecht, 1995.
[2] P. de Gennes, Introduction to Polymer Dynamics, Cambridge University Press, 1990.
[3] K. Sreenivasan, C. White, The onset of drag reduction by dilute polymer additives, and the maximum drag reduction asymptote, J. Fluid Mech. 409 (2000) 149–164.
[4] I. Radin, J.L. Zakin, G. Patterson, Drag reduction in solid–fluid systems, AIChE J. 21 (1975) 358–371.
[5] R.S. Kan, Drag reduction by particle addition, in: D.M. Bushnell, J.N. Hefner (Eds.), Viscous Drag Reduction in Boundary Layers, in: Progr. Astron. & Aeron, vol. 123, 1990, pp. 433–456.
[6] A.L. Moyls, R.H. Sabersky, Heat transfer and friction coefficients for dilute suspensions of asbestos fibers, Int. J. Heat Mass Transfer 21 (1978) 7–14.
[7] P. Virk, D. Wagger, Aspects of mechanisms in type B drag reduction, in: A. Gyr (Ed.), Structure of Turbulence and Drag Reduction, IUTAM Symp. Zürich, Switzerland, 1989, Springer, 1990, pp. 201–212.
[8] A. Einstein, Eine neue Bestimmung der Moleküldimension, Ann. Phys. 19 (1906) 289–306.
[9] A. Einstein, Berichtigung zu meiner Arbeit: "Eine neue Bestimmung der Moleküldimensionen", Ann. Phys. 34 (1911) 591–592.
[10] G. Jeffery, The motion of ellipsoidal particles immersed in a viscous fluid, Proc. Roy. Soc. London Ser. A 102 (1922) 161–179.
[11] H. Giesekus, Elasto-viskose Flüssigkeiten, für die in stationären Schichtströmungen sämtliche Normalspannungskomponenten verschieden groš sind, Rheol. Acta 2 (1962) 50–62.
[12] G. Batchelor, The stress system in a suspension of force-free particles, J. Fluid Mech. 41 (1970) 545–570.
[13] H. Brenner, Rheology of two-phase systems, Annu. Rev. Fluid Mech. 2 (1970) 137–176.
[14] H. Brenner, Suspension rheology in the presence of rotary brownian motion and external couples: elongational flow of dilute suspensions, Chem. Engrg. Sci. 27 (1972) 1069–1107.
[15] H. Brenner, Rheology of a dilute suspension of axisymmetric Brownian particles, Int. J. Multiphase Flow 1 (2) (1974) 195–341.
[16] L.G. Leal, E.J. Hinch, The rheology of a suspension of nearly spherical particles subjects to brownian rotations, J. Fluid Mech. 55 (1972) 745–765.
[17] E. Hinch, L. Leal, The effect of Brownian motion on the rheological properties of a suspension of non-spherical particles, J. Fluid Mech. 52 (1972) 683–712.
[18] E. Hinch, L. Leal, Constitutive equations in suspension mechanics. Part 1. General formulation, J. Fluid Mech. 71 (3) (1975) 481–495.
[19] E. Hinch, L. Leal, Constitutive equations in suspension mechanics. Part 2. Approximate forms for a suspension of rigid particles affected by Brownian rotations, J. Fluid Mech. 76 (1) (1976) 187–208.
[20] A. Okagawa, R. Cox, S. Mason, The kinetics of flowing disperions. VI. Transient orientation and rheological phenomena of rods and discs in shear flow, J. Colloid Interface Sci. 45 (2) (1973) 303–329.
[21] P. Frattini, G. Fuller, Rheo-optical studies of the effect of weak Brownian rotations in sheared suspensions, J. Fluid Mech. 168 (1986) 119–150.
[22] C. Stover, D. Koch, C. Cohen, Observations of fibre orientation in simple shear flow of semi-dilute suspensions, J. Fluid Mech. 238 (1992) 277–296.
[23] A. Szeri, L. Leal, A new computational method for the solution of flow problems of microstructured fluids. Part 1. Theory, J. Fluid Mech. 242 (1992) 549–576.
[24] A. Szeri, L. Leal, A new computational method for the solution of flow problems of microstructured fluids. Part 2. Inhomogeneous shear flow of a suspension, J. Fluid Mech. 262 (1994) 171–204.

[25] J. den Toonder, M. Hulsen, G. Kuiken, F. Nieuwstadt, Drag reduction by polymer additives in a turbulent pipe flow: numerical and laboratory experiments, J. Fluid Mech. 337 (1997) 193–231.
[26] M. Manhart, R. Friedrich, Direct numerical simulation of turbulent channel flow of a viscous anisotropic fluid, in: H.-J. Bungartz, R. Hoppe, C. Zenger (Eds.), Lectures on Applied Mathematics, Proceedings of the symposium organized by the SFB 438 "Mathematical Modelling, Simulation and Intelligent Systems" on the occasion of Karl-Heinz Hoffmann's 60th birthday, Munich, June 30–July 1, 1999, Springer, Heidelberg, 1999, pp. 277–296.
[27] R. Bird, C. Curtiss, R. Armstrong, O. Hassager, Kinetic Theory, second ed., in: Dynamics of Polymeric Liquids, vol. 2, Wiley, 1987.
[28] R. Sureshkumar, A. Beris, R. Handler, Direct numerical simulation of the turbulent channel flow of a polymer solution, Phys. Fluids 9 (3) (1997) 743–755.
[29] C. Dimitropoulos, R. Sureshkumar, A. Beris, Direct numerical simulation of viscoelastic turbulent channel flow exhibiting drag reduction: effect of the variation of rheological parameters, J. Non-Newtonian Fluid Mech. 79 (1998) 433–468.
[30] E. de Angelis, C.M. Casciola, R. Piva, Lagrangian tracking of polymers in wall turbulence, in: I.P. Castro, P.E. Hancock, T.G. Thomas (Eds.), Advances in Turbulence IX, Ninth European Turbulence Conference, CIMNE, Barcelona, 2002, pp. 373–376.
[31] E. de Angelis, C.M. Casciola, R. Piva, DNS of wall turbulence: dilute polymers and self-sustaining mechanisms, Comput. Fluids 31 (2002) 495–507.
[32] P.K. Ptasinski, F.T.M. Nieuwstadt, B.J. Boersma, Direct numerical simulations of viscoelastic turbulent channel flow close to maximum drag reduction, in: I.P. Castro, P.E. Hancock, T.G. Thomas (Eds.), Advances in Turbulence IX, Ninth European Turbulence Conference, CIMNE, Barcelona, 2002, pp. 89–92.
[33] M. Manhart, Rheology of suspensions of rigid-rod like particles in turbulent channel flow, J. Non-Newtonian Fluid Mech. (2003) in press.
[34] H. Öttinger, Stochastic Processes in Polymeric Fluids, Springer, Berlin, 1996.
[35] M. Doi, S. Edwards, The Theory of Polymer Dynamics, in: Internat. Ser. Monographs Phys., vol. 73, Oxford University Press, 1986.
[36] A.J. Chorin, Numerical solution of the Navier–Stokes equations, Math. Comput. 22 (1968) 745–762.
[37] R. Temam, On an approximate solution of the Navier–Stokes equations by the method of fractional steps. Part 1, Arch. Rational Mech. Anal. 32 (1969) 135–153.
[38] F.H. Harlow, J.E. Welsh, Numerical calculation of time-dependent viscous incompressible flow with free surface, Phys. Fluids 8 (1965) 2182–2189.
[39] A. Meri, H. Wengle, A.V.E. Dejoan, R. Schiestel, Applications of a 4th-order Hermitian scheme for non-equidistant grids to LES and DNS of incompressible fluid flow, in: E. Hirschel (Ed.), Notes Numer. Fluid Mech., vol. 66, Vieweg, Braunschweig, 1998, pp. 382–406.
[40] J. Kim, P. Moin, R. Moser, Turbulence statistics in fully developed channel flow at low Reynolds number, J. Fluid Mech. 177 (1987) 133–166.
[41] E.J. Hinch, Mechanical models of dilute polymer solutions in strong flows, Phys. Fluids 20 (10) (1977) S22–S30.